

The Underlying Event in Hard Scattering Processes

Rick Field^{1,*}

(for the CDF Collaboration)

¹ Department of Physics, University of Florida, Gainesville, Florida, 32611, USA

(Dated: October 27, 2018)

We study the behavior of the “underlying event” in hard scattering proton-antiproton collisions at 1.8 TeV and compare with the QCD Monte-Carlo models. The “underlying event” is everything except the two outgoing hard scattered “jets” and receives contributions from the “beam-beam remnants” plus initial and final-state radiation. The data indicate that neither ISAJET or HERWIG produce enough charged particles (with $p_T > 0.5$ GeV/c) from the “beam-beam remnant” component and that ISAJET produces too many charged particles from initial-state radiation. PYTHIA which uses multiple parton scattering to enhance the “underlying event” does the best job describing the data.

I. INTRODUCTION

FIG. 1 illustrates the way QCD Monte-Carlo models simulate a proton-antiproton collision in which a “hard” 2-to-2 parton scattering with transverse momentum, $p_T(\text{hard})$, has occurred. The resulting event contains particles that originate from the two outgoing partons (*plus initial and final-state radiation*) and particles that come from the breakup of the proton and antiproton (*i.e.*, “beam-beam remnants”). The “underlying event” is everything except the two outgoing hard scattered “jets” and receives contributions from the “beam-beam remnants” plus initial and final-state radiation. The “hard scattering” component consists of the outgoing two “jets” plus initial and final-state radiation.

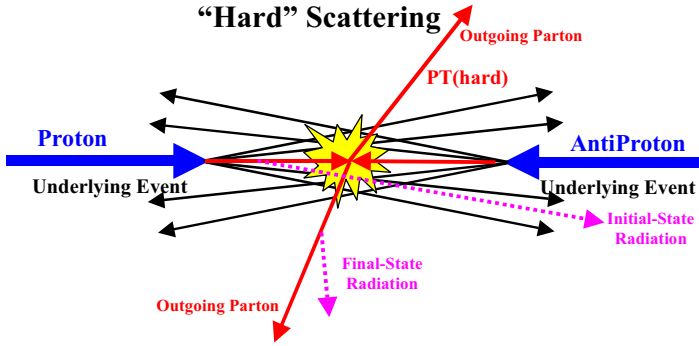


FIG. 1: Illustration of the way QCD Monte-Carlo models simulate a proton-antiproton collision in which a “hard” 2-to-2 parton scattering with transverse momentum, $p_T(\text{hard})$, has occurred. The resulting event contains particles that originate from the two outgoing partons (*plus initial and final-state radiation*) and particles that come from the breakup of the proton and antiproton (“beam-beam remnants”). The “underlying event” is everything except the two outgoing hard scattered “jets” and consists of the “beam-beam remnants” plus initial and final-state radiation. The “hard scattering” component consists of the outgoing two “jets” plus initial and final-state radiation.

The “beam-beam remnants” are what is left over after a parton is knocked out of each of the initial two beam hadrons. It is the reason hadron-hadron collisions are more “messy” than electron-positron annihilations and no one really knows how it should be modeled. For the QCD Monte-Carlo models the “beam-beam remnants” are an important component of the “underlying event”. Also, it is possible that multiple parton scattering contributes to the “underlying event”. FIG. 2 shows the way PYTHIA [1] models the “underlying event” in proton-antiproton collision by including multiple parton interactions. In addition to the hard 2-to-2 parton-parton scattering and the “beam-beam remnants”, sometimes there is a second “semi-hard” 2-to-2 parton-parton scattering that contributes particles to the “underlying event”.

*Talk presented at Snowmass 2001 (P5 working group); rfield@phys.ufl.edu; <http://www.phys.ufl.edu/~rfield/>

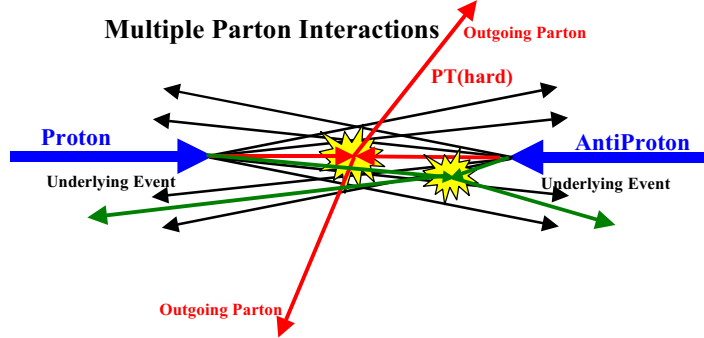


FIG. 2: Illustration of the way PYTHIA models the “underlying event” in proton-antiproton collision by including multiple parton interactions. In addition to the hard 2-to-2 parton-parton scattering with transverse momentum, $p_T(\text{hard})$, there is a second “semi-hard” 2-to-2 parton-parton scattering that contributes particles to the “underlying event”.

Of course, from a certain point of view there is no such thing as an “underlying event” in a proton-antiproton collision. There is only an “event” and one cannot say where a given particle in the event originated. On the other hand, hard scattering collider “jet” events have a distinct topology. On the average, the outgoing hadrons “remember” the underlying the 2-to-2 hard scattering subprocess. An average hard scattering event consists of a collection (or burst) of hadrons traveling roughly in the direction of the initial beam particles and two collections of hadrons (*i.e.*, “jets”) with large transverse momentum. The two large transverse momentum “jets” are roughly back to back in azimuthal angle. One can use the topological structure of hadron-hadron collisions to study the “underlying event” [2, 3, 4]. The ultimate goal is to understand the physics of the “underlying event”, but since it is very complicated and involves both non-perturbative as well as perturbative QCD it seems unlikely that this will happen soon. In the mean time, we would like to tune the QCD Monte-Carlo models to do a better job fitting the “underlying event”. The “underlying event” is an unavoidable background to most collider observables. To find “new” physics at a collider it is crucial to have Monte-Carlo models that simulate accurately “ordinary” hard-scattering collider events. In this talk I will compare collider observables that are sensitive to the “underlying event” with the QCD Monte-Carlo model predictions of PYTHIA 6.115 [1], HERWIG 5.9 [5], and ISAJET 7.32 [6] and discuss the tuning of PYTHIA.

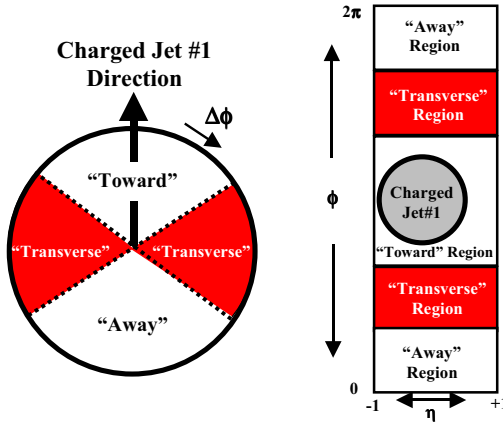


FIG. 3: Illustration of correlations in azimuthal angle $\Delta\phi$ relative to the direction of the leading charged jet in the event, chgjet#1. The angle $\Delta\phi = \phi - \phi_{\text{chgjet}\#1}$ is the relative azimuthal angle between charged particles and the direction of chgjet#1. The “toward” region is defined by $|\Delta\phi| < 60^\circ$ and $|\eta| < 1$, while the “away” region is $|\Delta\phi| > 120^\circ$ and $|\eta| < 1$. The “transverse” region is defined by $60^\circ < |\Delta\phi| < 120^\circ$ and $|\eta| < 1$. Each region has an area in η - ϕ space of $4\pi/3$.

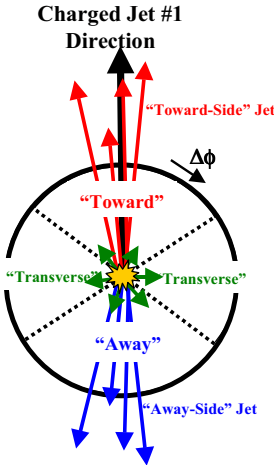


FIG. 4: Illustration of the topology of an average proton-antiproton collision in which a “hard” 2-to-2 parton scattering has occurred. The “toward” region as defined in FIG. 3 contains the leading charged particle “jet”, while the “away” region, on the average, contains the “away-side” jet. The “transverse” region is perpendicular to the plane of the hard 2-to-2 scattering and is very sensitive to the “underlying event”.

II. THE “TRANSVERSE” REGION

In a proton-antiproton collision large transverse momentum outgoing partons manifest themselves, in the laboratory, as a clusters of particles (*both charged and neutral*) traveling in roughly the same direction. These clusters are referred to as “jets”. In this analysis we examine only the charged particle component of “jets”. Our philosophy in comparing the QCD Monte-Carlo models with data is to select a region where the data is very “clean” so that “what you see is what you get” (*almost*). Hence, we consider only charged particles measured by the CDF central tracking chamber (CTC) in the region $p_T > 0.5 \text{ GeV}/c$ and $|\eta| < 1$, where the track finding efficiency is high and uniform (estimated to be 92% efficient) and we restrict ourselves to charged particle jets with transverse momentum less than 50 GeV/c. The data presented here are uncorrected. Instead the theoretical Monte-Carlo models are corrected for the track finding efficiency by removing, on the average, 8% of the charged particles. The theory curves have an error (*statistical plus systematic*) of about 5%. Thus, to within 10% “what you see is what you get”.

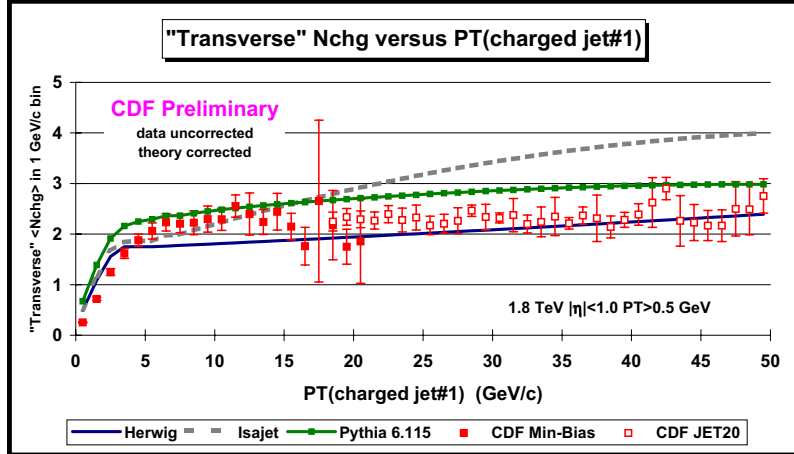


FIG. 5: Data on the average number of charged particles ($p_T > 0.5 \text{ GeV}/c$, $|\eta| < 1$) in the “transverse region” defined in FIG. 3 as a function of transverse momentum of the leading charged jet compared with the QCD Monte-Carlo predictions of HERWIG 5.9, ISAJET 7.32, and PYTHIA 6.115 with their default parameters and with $p_T(\text{hard}) > 3 \text{ GeV}/c$. Each point corresponds to the $\langle N_{\text{chq}} \rangle$ in a $1 \text{ GeV}/c$ bin. The solid (open) points are the Min-Bias (JET20) data. The theory curves are corrected for the track finding efficiency and have an error (*statistical plus systematic*) of around 5%.

Charged particle “jets” are defined as clusters of charged particles ($p_T > 0.5 \text{ GeV}/c$, $|\eta| < 1$) in “circular

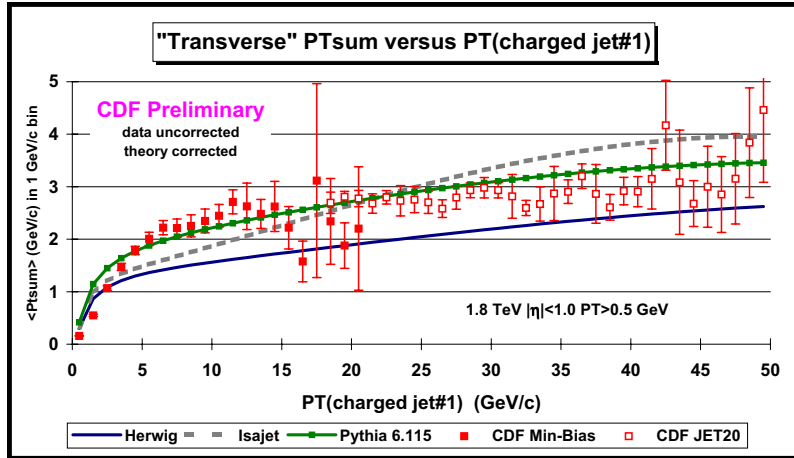


FIG. 6: Data on the average *scalar p_T* sum of charged particles ($p_T > 0.5 \text{ GeV}/c$, $|\eta| < 1$) in the “transverse” region defined in FIG. 3 as a function of the transverse momentum of the leading charged jet compared with the QCD Monte-Carlo predictions of HERWIG 5.9, ISAJET 7.32, and PYTHIA 6.115 with their default parameters and with $p_T(\text{hard}) > 3 \text{ GeV}/c$. Each point corresponds to the $\langle P_{T\text{sum}} \rangle$ in a 1 GeV/c bin. The solid (open) points are the Min-Bias (JET20) data. The theory curves are corrected for the track finding efficiency and have an error (*statistical plus systematic*) of around 5%.

regions” of η - ϕ space with radius $R = 0.7$. Every charged particle in the event is assigned to a “jet”, with the possibility that some jets might consist of just one charged particle. The transverse momentum of a charged jet, $P_T(\text{chjet})$, is the *scalar p_T* sum of the particles in the jet. We use the direction of the leading charged particle jet to define correlations in azimuthal angle, $\Delta\phi$. The angle $\Delta\phi = \phi - \phi_{\text{chjet}\#1}$ is the relative azimuthal angle between a charged particle and the direction of chjet#1. The “toward” region is defined by $|\Delta\phi| < 60^\circ$ and $|\eta| < 1$, while the “away” region is $|\Delta\phi| > 120^\circ$ and $|\eta| < 1$. The “transverse” region is defined by $60^\circ < |\Delta\phi| < 120^\circ$ and $|\eta| < 1$. The three regions “toward”, “transverse”, and “away” are shown in FIG. 3. Each region has an area in η - ϕ space of $4\pi/3$. As illustrated in FIG. 4, the “toward” region contains the leading charged particle jet, while the “away” region, on the average, contains the “away-side” jet. The “transverse” region is perpendicular to the plane of the hard 2-to-2 scattering and is therefore very sensitive to the “underlying event”.

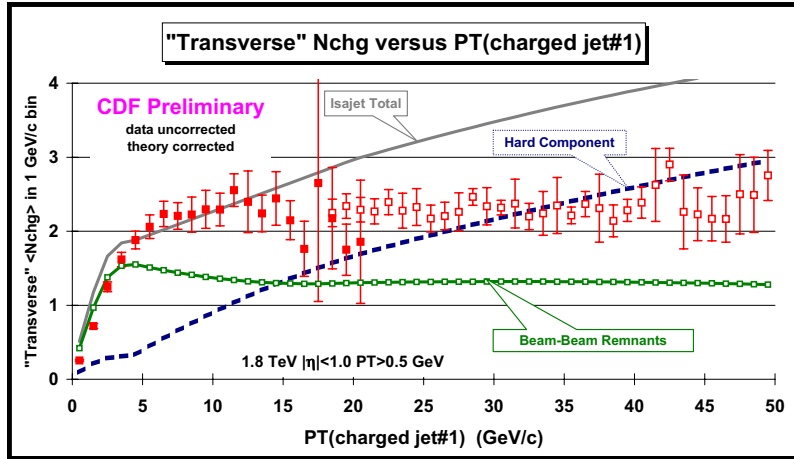


FIG. 7: Data on the average number of charged particles ($p_T > 0.5 \text{ GeV}/c$, $|\eta| < 1$) in the “transverse” region defined in FIG. 3 as a function of the transverse momentum of the leading charged jet compared with the QCD Monte-Carlo predictions of ISAJET 7.32 (default parameters and $p_T(\text{hard}) > 3 \text{ GeV}/c$). The predictions of ISAJET are divided into two categories: charged particles that arise from the break-up of the beam and target (*beam-beam remnants*), and charged particles that result from the outgoing jets plus initial and final-state radiation (*hard scattering component*). The theory curves are corrected for the track finding efficiency and have an error (*statistical plus systematic*) of around 5%.

FIG. 5 and FIG. 6 compare the “transverse” $\langle N_{\text{ch}} \rangle$ and the “transverse” $\langle P_{T\text{sum}} \rangle$, respectively, with the

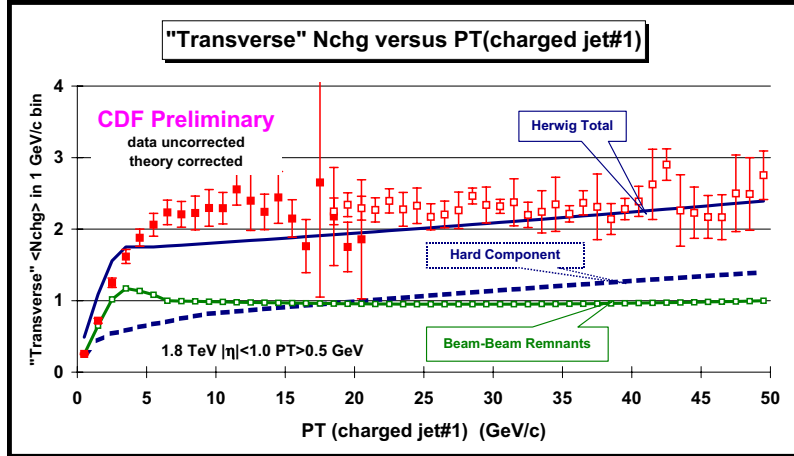


FIG. 8: Data on the average number of charged particles ($p_T > 0.5 \text{ GeV}/c$, $|\eta| < 1$) in the “transverse” region defined in FIG. 3 as a function of the transverse momentum of the leading charged jet compared with the QCD Monte-Carlo predictions of HERWIG 5.9 (default parameters and $p_T(\text{hard}) > 3 \text{ GeV}/c$). The predictions of HERWIG are divided into two categories: charged particles that arise from the break-up of the beam and target (*beam-beam remnants*), and charged particles that result from the outgoing jets plus initial and final-state radiation (*hard scattering component*). The theory curves are corrected for the track finding efficiency and have an error (*statistical plus systematic*) of around 5%.

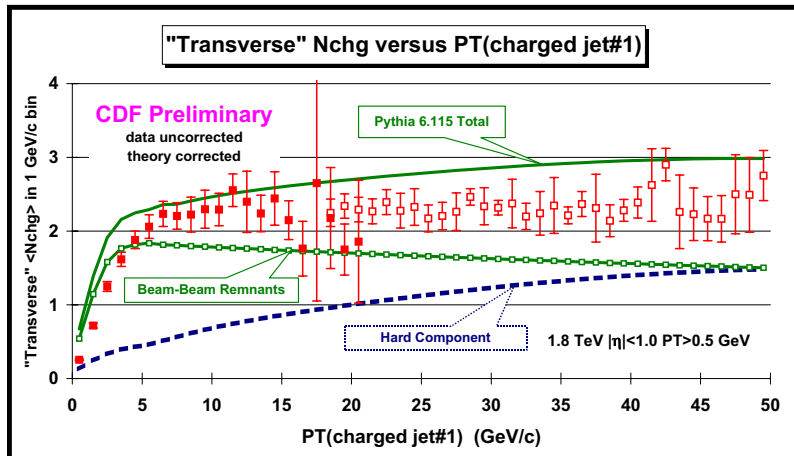


FIG. 9: Data on the average number of charged particles ($p_T > 0.5 \text{ GeV}/c$, $|\eta| < 1$) in the “transverse” region defined in FIG. 3 as a function of the transverse momentum of the leading charged jet compared with the QCD Monte-Carlo predictions of PYTHIA 6.115 (default parameters and $p_T(\text{hard}) > 3 \text{ GeV}/c$). The predictions of PYTHIA are divided into two categories: charged particles that arise from the break-up of the beam and target (*beam-beam remnants*), and charged particles that result from the outgoing jets plus initial and final-state radiation (*hard scattering component*). For PYTHIA the “beam-beam remnants” include contributions from multiple parton scattering. The theory curves are corrected for the track finding efficiency and have an error (*statistical plus systematic*) of around 5%.

QCD Monte-Carlo predictions of HERWIG, ISAJET, and PYTHIA 6.115 with their default parameters and $p_T(\text{hard}) > 3 \text{ GeV}/c$. The solid points are Min-Bias data and the open points are the JET20 data. The JET20 data connect smoothly to the Min-Bias data and allow us to study observables over the range $0.5 < p_T(\text{chjet}\#1) < 50 \text{ GeV}/c$. The average number of charged particles in the “transverse” region doubles in going from $p_T(\text{chjet}\#1) = 1.5 \text{ GeV}/c$ to $2.5 \text{ GeV}/c$ and then forms an approximately constant “plateau” for $p_T(\text{chjet}\#1) > 5 \text{ GeV}/c$. If we suppose that the “underlying event” is uniform in azimuthal angle ϕ and pseudo-rapidity η , the observed 2.3 charged particles at $p_T(\text{chjet}\#1) = 20 \text{ GeV}/c$ translates to 3.8 charged particles per unit pseudo-rapidity with $p_T > 0.5 \text{ GeV}/c$ (multiply by 3 to get 360° , divide by 2 for the two units of pseudo-rapidity, multiply by 1.09 to correct for the track finding efficiency). We know that if we include all $p_T > 50 \text{ MeV}/c$ there are, on the average, about four charged particles per unit rapidity in a “soft” proton-antiproton collision at 1.8 TeV [7]. The data in FIG. 5 imply that in the “underlying event” of a hard scattering there are,

on the average, about 3.8 charged particles per unit rapidity with $p_T > 0.5 \text{ GeV}/c$! Assuming a charged particle p_T distribution of e^{-2p_T} (see FIG. 17) implies that there are roughly 10 charged particles per unit pseudo-rapidity with $p_T > 0$ in the “underlying event” (factor of e). Since we examine only those charge particles with $p_T > 0.5 \text{ GeV}/c$, we cannot accurately extrapolate to low p_T , however, it is clear that the “underlying event” has a charge particle density that is at least a factor of two larger than the four charged particles per unit rapidity seen in “soft” proton-antiproton collisions at this energy.

The Min-Bias data were collected with a very “loose” trigger. The CDF Min-Bias trigger requirement removes elastic scattering and most of the single and double diffraction events, but keeps essentially all the “hard-scattering” events. In comparing with the QCD Monte-Carlo models we do require that the models satisfy the CDF Min-Bias trigger, however, for $P_T(\text{chgjet}\#1) > 5 \text{ GeV}/c$ essentially all the generated events satisfy the Min-Bias trigger (*i.e.*, the Min-Bias trigger is unbiased for large p_T “jets”). If we had enough Min-Bias events we would not need the JET20 data, but because of the fast fall-off of the cross section we run out of statistics at around $P_T(\text{chgjet}\#1) = 20 \text{ GeV}/c$ (that is why the Min-Bias data errors get large at around $20 \text{ GeV}/c$). The JET20 data were collected by requiring at least 20 GeV of energy (*charged plus neutral*) in a cluster of calorimeter cells. We do not use the calorimeter information, but instead look only at the charged particles measured in the CTC in the same way we do for the Min-Bias data. The JET20 data is, of course, biased for low p_T jets and we do not show the JET20 data below $P_T(\text{chgjet}\#1)$ around $20 \text{ GeV}/c$. At large $P_T(\text{chgjet}\#1)$ values the JET20 data becomes unbiased and, in fact, we know this occurs at around $20 \text{ GeV}/c$ because it is here that it agrees with the (*unbiased*) Min-Bias data.

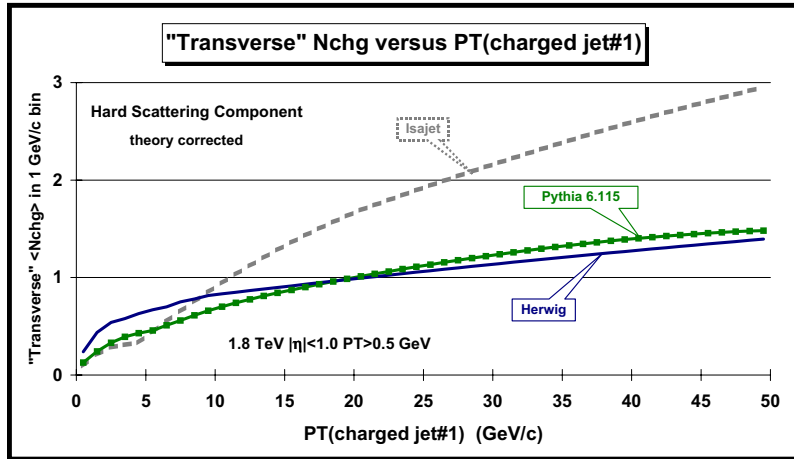


FIG. 10: The “hard scattering” component (*outgoing jets plus initial and final-state radiation*) of the number of charged particles ($p_T > 0.5 \text{ GeV}/c$, $|\eta| < 1$) in the “transverse” region defined in FIG. 3 as a function of the transverse momentum of the leading charged jet from the QCD Monte-Carlo predictions of HERWIG 5.9, ISAJET 7.32, and PYTHIA 6.115 with their default parameters and with $p_T(\text{hard}) > 3 \text{ GeV}/c$. The curves are corrected for the track finding efficiency and have an error (*statistical plus systematic*) of around 5%.

We expect the “transverse” region to be composed predominately of particles that arise from the break-up of the beam and target and from initial and final-state radiation. This is clearly the case for the QCD Monte-Carlo models as can be seen in FIGS. 7-9, where the predictions for the “transverse” region are divided into two categories: charged particles that arise from the break-up of the beam and target (*beam-beam remnants*), and charged particles that result from the outgoing jets plus initial and final-state radiation (*hard scattering component*). For PYTHIA the “beam-beam remnant” contribution includes contributions from multiple parton scattering. It is interesting to see that in the QCD Monte-Carlo models it is the “beam-beam remnants” that are producing the approximately constant “plateau”. The contributions from initial-state and final-state radiation increase as $P_T(\text{chgjet}\#1)$ increases. In fact, for ISAJET it is the sharp rise in the initial-state radiation component that is causing the disagreement with the data for $P_T(\text{chgjet}\#1) > 20 \text{ GeV}/c$. The hard scattering component of HERWIG and PYTHIA does not rise nearly as fast as the hard scattering component of ISAJET.

There are two reasons why the hard scattering component of ISAJET is different from HERWIG and PYTHIA. The first is due to different fragmentation schemes. ISAJET uses independent fragmentation, which produces too many soft hadrons when partons begin to overlap. The second difference arises from the way the QCD Monte-Carlo produce “parton showers”. ISAJET uses a leading-log picture in which the partons within the shower are ordered according to their invariant mass. Kinematics requires that the invariant mass of daughter partons be less than the invariant mass of the parent. HERWIG and PYTHIA modify the leading-log picture to include “color coherence effects” which leads to “angle ordering” within the parton shower. Angle ordering

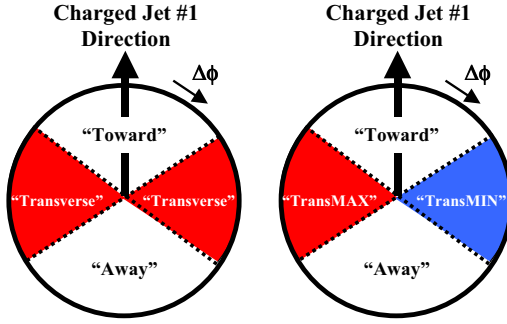


FIG. 11: Illustration of correlations in azimuthal angle $\Delta\phi$ relative to the direction of the leading charged jet in the event, chgjet#1. The angle $\Delta\phi = \phi - \phi_{\text{chgjet}\#1}$ is the relative azimuthal angle between charged particles and the direction of chgjet#1. On an event by event basis, we define “transMAX” (“transMIN”) to be the maximum (minimum) of the two “transverse” pieces, $60^\circ < \Delta\phi < 120^\circ$ and $|\eta| < 1$, and $60^\circ < -\Delta\phi < 120^\circ$ and $|\eta| < 1$. “TransMAX” and “transMIN” each have an area in $\eta\text{-}\phi$ space of $2\pi/3$. The sum of “TransMAX” and “transMIN” is the total “transverse” region with area $4\pi/3$.

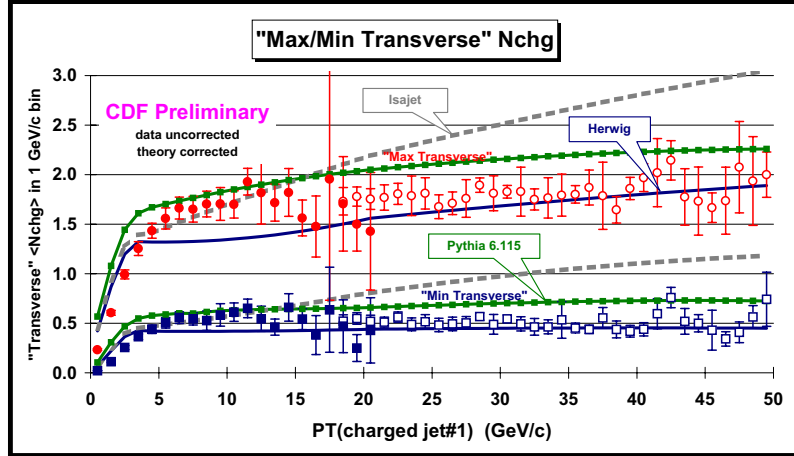


FIG. 12: Data on the average number of “transMAX” and “transMIN” charged particles ($p_T > 0.5 \text{ GeV}/c$, $|\eta| < 1$) as a function of the transverse momentum of the leading charged jet compared with the QCD Monte-Carlo predictions of HERWIG 5.9, ISAJET 7.32, and PYTHIA 6.115 with their default parameters and with $p_T(\text{hard}) > 3 \text{ GeV}/c$. The solid (open) points are the Min-Bias (JET20) data. The theory curves are corrected for the track finding efficiency and have an error (statistical plus systematic) of around 5%.

produces less high p_T radiation within a parton shower which is what is seen in FIG. 10.

Of course, the origin of an outgoing particle (“beam-beam remnant” or “hard-scattering”) is not an experimental observable. Experimentally one cannot say where a given particle comes from. However, we do know the origins of particles generated by the QCD Monte-Carlo models and FIGS. 7-9 show the composition of the “transverse” region as predicted by ISAJET, HERWIG, and PYTHIA.

III. MAXIMUM AND MINIMUM “TRANSVERSE” REGIONS

We now break up the “transverse” region into two pieces. As illustrated in FIG. 11, on an event by event basis, we define “transMAX” (“transMIN”) to be the maximum (minimum) of the two “transverse” pieces, $60^\circ < \Delta\phi < 120^\circ$, $|\eta| < 1$, and $60^\circ < -\Delta\phi < 120^\circ$, $|\eta| < 1$. Each has an area in $\eta\text{-}\phi$ space of $2\pi/3$ and what we previously referred to as the “transverse” region is the sum of “transMAX” and “transMIN”. One expects that “transMAX” will pick up more of the initial and final state radiation while “transMIN” should be more sensitive to the “beam-beam remnant” component of the “underlying event”. Furthermore, one expects that the “beam-beam remnant” component will nearly cancel in the difference, “transMAX” minus “transMIN”. If this is true then the difference, “transMAX” minus “transMIN”, would be more sensitive to the “hard scattering” component (*i.e.*, initial and final-state radiation). I believe that this idea was first proposed by Bryan Webber

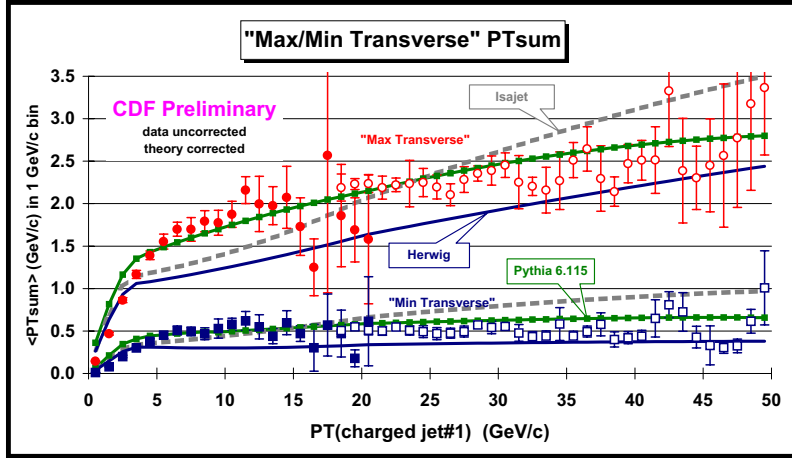


FIG. 13: Data on the average scalar p_T sum of the “transMAX” and “transMIN” charged particles ($p_T > 0.5$ GeV/c, $|\eta| < 1$) as a function of the transverse momentum of the leading charged jet compared with the QCD Monte-Carlo predictions HERWIG 5.9, ISAJET 7.32, and PYTHIA 6.115 with their default parameters and with $p_T(\text{hard}) > 3$ GeV/c. The solid (open) points are the Min-Bias (JET20) data. The theory curves are corrected for the track finding efficiency and have an error (statistical plus systematic) of around 5%.

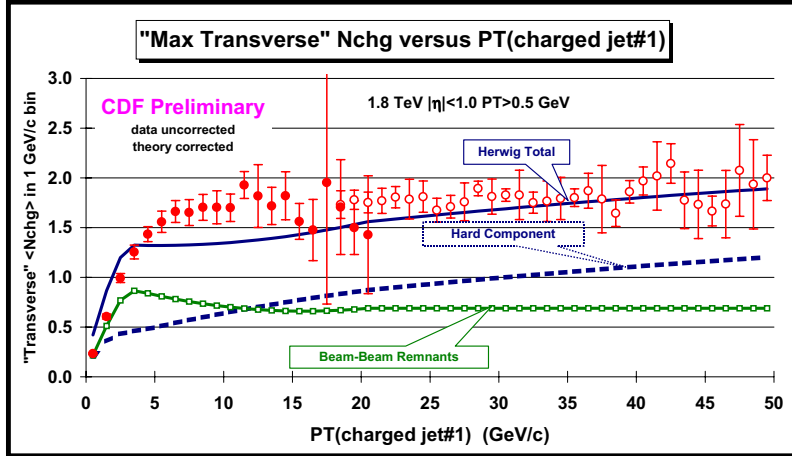


FIG. 14: Data on the average number of “transMAX” charged particles ($p_T > 0.5$ GeV/c, $|\eta| < 1$) as a function of the transverse momentum of the leading charged jet compared with the QCD Monte-Carlo predictions of HERWIG 5.9 (default parameters and $p_T(\text{hard}) > 3$ GeV/c). The predictions of HERWIG are divided into two categories: charged particles that arise from the break-up of the beam and target (*beam-beam remnants*), and charged particles that result from the outgoing jets plus initial and final-state radiation (*hard scattering component*). The theory curves are corrected for the track finding efficiency and have an error (statistical plus systematic) of around 5%.

and then implemented in a paper by Jon Pumplin [8].

FIG. 12 and FIG. 13 show the data on the $\langle N_{\text{chg}} \rangle$ and $\langle P_{\text{Tsum}} \rangle$, respectively, for the “transMAX” and “transMIN” region as a function of the $P_T(\text{chjet}\#1)$ compared with QCD Monte-Carlo predictions of HERWIG, ISAJET, and PYTHIA with their default parameters and $p_T(\text{hard}) > 3$ GeV/c. FIG. 14, FIG. 15, and FIG. 16 show the data on $\langle N_{\text{chg}} \rangle$ for “transMAX”, “transMIN”, and the difference “transMAX” minus “transMIN”, respectively, compared with QCD Monte-Carlo predictions of HERWIG. The predictions of HERWIG are divided into two categories: charged particles that arise from the break-up of the beam and target (*beam-beam remnants*), and charged particles that result from the outgoing jets plus initial and final-state radiation (*hard scattering component*). It is clear from these plots that in the QCD Monte-Carlo models the “transMAX” is more sensitive to the “hard scattering component” of the “underlying event” while “transMIN” is more sensitive to the “beam-beam remnants”, especially at large values of $P_T(\text{chjet}\#1)$. For example, for HERWIG at $P_T(\text{chjet}\#1) = 40$ GeV/c the hard scattering component makes up 62% of the “transMAX” $\langle N_{\text{chg}} \rangle$ with 38% coming from the “beam-beam remnants”. On the other hand, the hard scattering component makes up only 42% of the “transMIN” $\langle N_{\text{chg}} \rangle$ with 58% coming from the “beam-beam remnants” at $P_T(\text{chjet}\#1) = 40$ GeV/c.

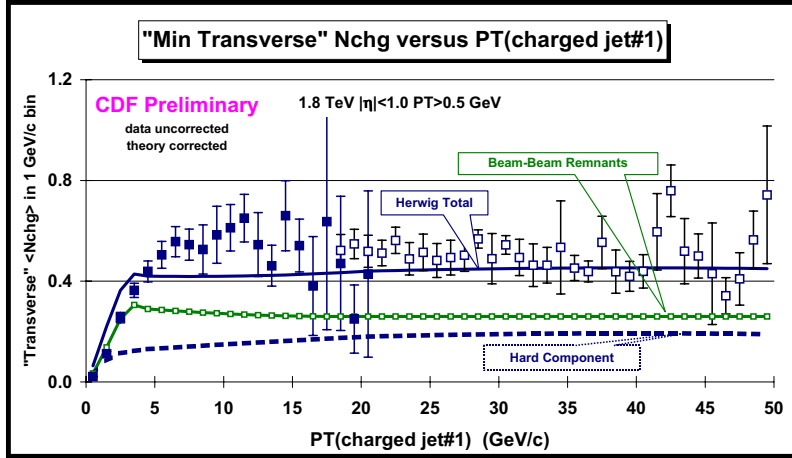


FIG. 15: Data on the average number of “transMIN” charged particles ($p_T > 0.5 \text{ GeV}/c$, $|\eta| < 1$) as a function of the transverse momentum of the leading charged jet compared with the QCD Monte-Carlo predictions of HERWIG 5.9 (default parameters and $p_T(\text{hard}) > 3 \text{ GeV}/c$). The predictions of HERWIG are divided into two categories: charged particles that arise from the break-up of the beam and target (*beam-beam remnants*), and charged particles that result from the outgoing jets plus initial and final-state radiation (*hard scattering component*). The theory curves are corrected for the track finding efficiency and have an error (*statistical plus systematic*) of around 5%.

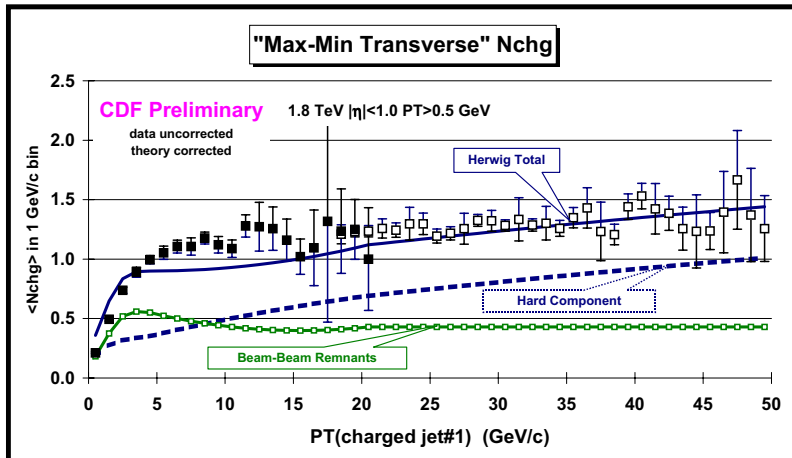


FIG. 16: Data on the average difference “transMAX” minus “transMIN”, for the number of charged particles ($p_T > 0.5 \text{ GeV}/c$, $|\eta| < 1$) as a function of the transverse momentum of the leading charged jet compared with the QCD Monte-Carlo predictions of HERWIG 5.9 (default parameters and $p_T(\text{hard}) > 3 \text{ GeV}/c$). The predictions of HERWIG are divided into two categories: charged particles that arise from the break-up of the beam and target (*beam-beam remnants*), and charged particles that result from the outgoing jets plus initial and final-state radiation (*hard scattering component*). The theory curves are corrected for the track finding efficiency and have an error (*statistical plus systematic*) of around 5%.

Taking difference between “transMAX” and “transMIN” does not completely remove the “beam-beam remnant” component, but reduces it to only about 32% at $P_T(\text{chqjet}\#1) = 40 \text{ GeV}/c$.

IV. THE TRANSVERSE MOMENTUM DISTRIBUTION IN THE “TRANSVERSE” REGION

FIG. 17 shows the data on the transverse momentum distribution of charged particles in the “transverse” region for $P_T(\text{chqjet}\#1) > 2 \text{ GeV}/c$, $5 \text{ GeV}/c$, and $30 \text{ GeV}/c$. Each point corresponds to dN_{chg}/dp_T and the integral of the distribution gives the average number of charged particles in the “transverse” region, $\langle N_{\text{chg}} \rangle$, shown in FIG. 5. FIG. 5 shows only mean values, while FIG. 17 shows the distribution from which the mean is computed. The data are compared with the QCD hard scattering Monte-Carlo models predictions HERWIG. Since these distributions fall off sharply as p_T increases, it is essentially only the first few points at low p_T that

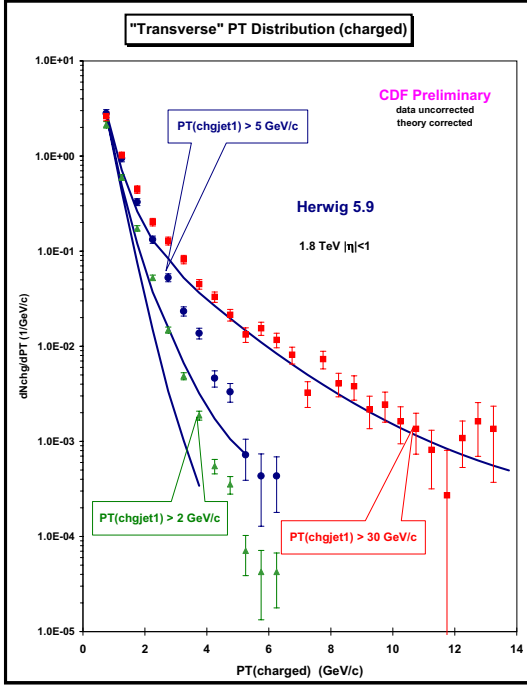


FIG. 17: Data on the transverse momentum distribution of charged particles ($p_T > 0.5 \text{ GeV}/c$, $|\eta| < 1$) in the “transverse” region for $P_T(\text{chgjet}\#1) > 2 \text{ GeV}/c$, $5 \text{ GeV}/c$, and $30 \text{ GeV}/c$, where chgjet $\#1$ is the leading charged particle jet. Each point corresponds to dN_{chg}/dp_T and the integral of the distribution gives the average number of charged particles in the transverse region, $\langle N_{\text{chg}}(\text{transverse}) \rangle$. The data are compared with the QCD Monte-Carlo model predictions of HERWIG 5.9 (default parameters and $p_T(\text{hard}) > 3 \text{ GeV}/c$). The theory curves are corrected for the track finding efficiency and have an error (*statistical plus systematic*) of around 5%.

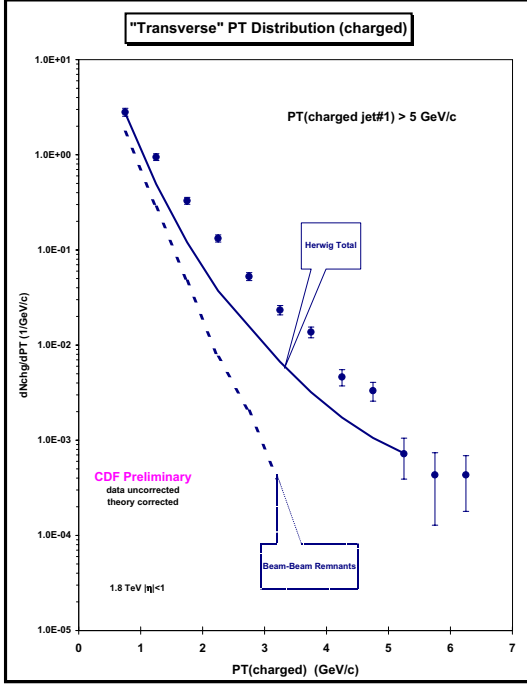


FIG. 18: Data on the transverse momentum distribution of charged particles ($p_T > 0.5 \text{ GeV}/c$, $|\eta| < 1$) in the “transverse” region for $P_T(\text{chgjet}\#1) > 5 \text{ GeV}/c$ compared with the QCD Monte-Carlo model predictions of HERWIG 5.9 (default parameters and $p_T(\text{hard}) > 3 \text{ GeV}/c$). The theory curves are corrected for the track finding efficiency and have an error (*statistical plus systematic*) of around 5%. The solid curve is the total (“hard scattering” plus “beam-beam remnants”) and the dashed curve shows the contribution arising from the break-up of the beam particles (“beam-beam remnants”).

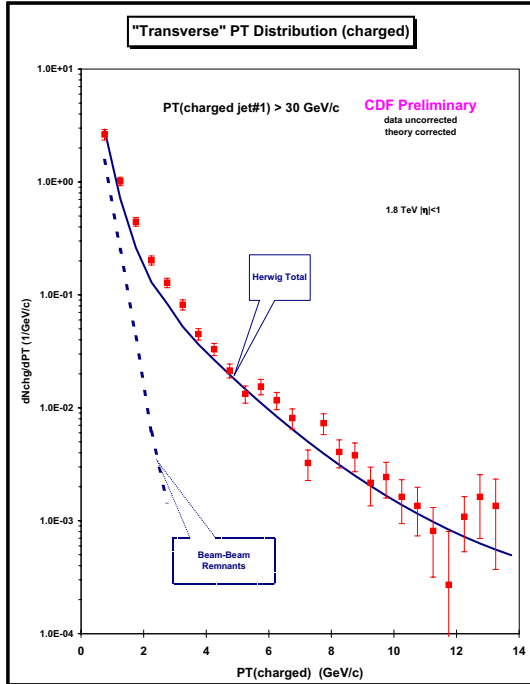


FIG. 19: Data on the transverse momentum distribution of charged particles ($p_T > 0.5 \text{ GeV}/c$, $|\eta| < 1$) in the “transverse” region for $P_T(\text{chjet}\#1) > 30 \text{ GeV}/c$ compared with the QCD Monte-Carlo model predictions of HERWIG 5.9 (default parameters and $p_T(\text{hard}) > 3 \text{ GeV}/c$). The theory curves are corrected for the track finding efficiency and have an error (*statistical plus systematic*) of around 5%. The solid curve is the total (“hard scattering” plus “beam-beam remnants”) and the dashed curve shows the contribution arising from the break-up of the beam particles (“beam-beam remnants”).

determine the mean. The approximately constant plateau seen in FIG. 5 is a result of the low p_T points in FIG. 17 not changing much as $P_T(\text{chjet}\#1)$ changes. However, the high p_T points do increase considerably as $P_T(\text{chjet}\#1)$ increases. This effect cannot be seen by simply examining the average number of “transverse” particles. FIG. 17 shows the growth of the “hard scattering component” at large p_T in the “transverse region” (*i.e.*, three or more hard scattering jets). For the QCD Monte-Carlo models the p_T distribution in the “transverse” region, at low values of $P_T(\text{chjet}\#1)$, is dominated by the “beam-beam remnant” contribution with very little “hard scattering” component. This can be seen in FIG. 18 which shows both the “beam-beam remnant” component together with the total overall prediction of HERWIG for $P_T(\text{chjet}\#1) > 5 \text{ GeV}/c$. For the QCD Monte-Carlo models the p_T distribution in the “transverse” region, at low values of $P_T(\text{chjet}\#1)$, measures directly the p_T distribution of the “beam-beam remnants”. Both ISAJET and HERWIG have the wrong p_T dependence in the “transverse” region due to a “beam-beam remnant” component that falls off too rapidly as p_T increases. It is, of course, understandable that the Monte-Carlo models might be slightly off on the parameterization of the “beam-beam remnants”. This component cannot be calculated from perturbation theory and must be determined from data.

FIG. 19 shows both the “beam-beam remnant” component together with the overall prediction of HERWIG for $P_T(\text{chjet}\#1) > 30 \text{ GeV}/c$. Here the QCD Monte-Carlo models predict a large “hard scattering” component corresponding to the production of more than two large p_T jets. HERWIG, ISAJET, and PYTHIA all do well at describing the high p_T tail of this distribution.

V. “TRANSVERSE REGIONS” VERSUS “TRANSVERSE CONES”

In a complementary CDF analysis Valeria Tano [4] has studied the “underlying event” in hard scattering processes by defining “transverse cones” instead of “transverse regions”. As illustrated in FIG. 20, the “transverse cones” (with radius in η - ϕ space of $R = 0.7$) are located at the same pseudo-rapidity as the leading jet but with azimuthal angle $\Delta\phi = +90^\circ$ and $\Delta\phi = -90^\circ$ relative to the leading “jet”. In the cone analysis the “jet” is a “calorimeter jet” (*charged plus neutrals*) defined using the standard CDF cluster algorithm. Maximum (MAX) and minimum (MIN) “transverse” cones are determined, on an event-by-event basis, similar to the “trans-MAX” and “transMIN” regions described in Section III. Each “transverse cone” has an area in η - ϕ space of

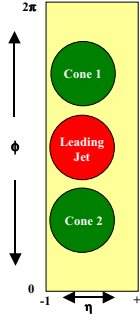


FIG. 20: Illustration of “transverse cones” with radius in η - ϕ space of $R = 0.7$ which are located at the same pseudorapidity as the leading jet but with azimuthal angle $\Delta\phi = +90^\circ$ and $\Delta\phi = -90^\circ$ relative to the leading jet. Each “transverse cone” has an area in η - ϕ space of $\pi R^2 = 0.49\pi$.

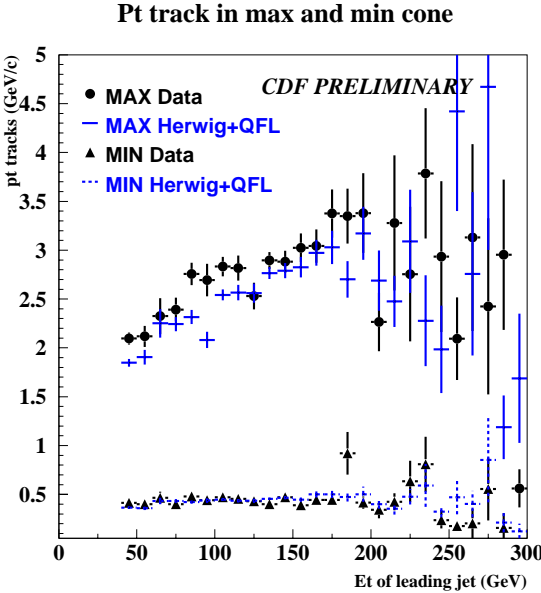


FIG. 21: Data on the average *scalar* p_T sum of charged particles ($p_T > 0.4$ GeV/c, $|\eta| < 1$) within the maximum (MAX) and minimum (MIN) “transverse cones” defined in FIG. 20 versus the transverse energy of the leading (*highest* E_T) “calorimeter jet” compared with the QCD Monte-Carlo model predictions HERWIG 5.9 (*default parameters*).

$\pi R^2 = 0.49\pi$ (compared with 0.67π). FIG. 21 shows data at 1.8 TeV on the average *scalar* p_T sum of charged particles ($p_T > 0.4$ GeV/c, $|\eta| < 1$) within the MAX and MIN “transverse cones” versus the transverse energy of the leading (*highest* E_T) “calorimeter jet” compared with the QCD hard scattering Monte-Carlo models predictions HERWIG. The “transverse cone” analysis covers the range $50 < E_T(\text{calorimeter jet}\#1) < 300$ GeV, while the “transverse region” analysis examines only charged particles and covers the range $0 < P_T(\text{chgjet}\#1) < 50$ GeV/c. One cannot directly compare the two analysis, but if one scales the low $E_T(\text{jet}\#1)$ points in FIG. 21 by the ratio of areas $0.67\pi/0.49\pi = 1.36$, one gets approximate agreement with the high $P_T(\text{chgjet}\#1)$ points in FIG. 13. Both FIG. 13 and FIG. 21 indicate that the $\langle P_{T\text{sum}} \rangle$ of charged particles generated by HERWIG is slightly too small. Together the two CDF analyses give us a good handle on the “underlying event” in hard scattering processes.

VI. TUNING PYTHIA TO FIT THE “UNDERLYING EVENT”

Now that we have constructed collider observables that are sensitive to the “underlying event” we would like to tune the multiple parton interaction parameters of PYTHIA to fit the data. There are many tunable parameters. Here we consider only the parameters given in Table I. The default values of the parameters are given in Table II. Note that the PYTHIA default values sometimes change as the version changes [9].

TABLE I: PYTHIA multiple parton scattering parameters.

Parameter	Value	Description
MSTP(81)	0	Multiple-Parton Scattering off
	1	Multiple-Parton Scattering on
MSTP(82)	1	Multiple interactions assuming the same probability, with an abrupt cut-off $P_{T\min}=\text{PARP}(81)$
	3	Multiple interactions assuming a varying impact parameter and a hadronic matter overlap consistent with a single Gaussian matter distribution, with a smooth turn-off $P_{T0}=\text{PARP}(82)$
	4	Multiple interactions assuming a varying impact parameter and a hadronic matter overlap consistent with a double Gaussian matter distribution (governed by PARP(83) and PARP(84)) with a smooth turn-off $P_{T0}=\text{PARP}(82)$

TABLE II: Default values for some of the multiple parton scattering parameters of PYTHIA.

Parameter	PYTHIA 6.115	PYTHIA 6.125
MSTP(81)	1	1
MSTP(82)	1	1
PARP(81)	1.4 GeV/c	1.9 GeV/c
PARP(82)	1.55 GeV/c	2.1 GeV/c
PARP(83)	0.5	0.5
PARP(84)	0.2	0.2

FIG. 22 and FIG. 23 show data on the average number of charged particles in the “transverse” region compared with the QCD Monte-Carlo predictions of PYTHIA 6.115 with different structure functions and different multiple parton interaction parameters and with $p_T(\text{hard}) > 0 \text{ GeV}/c$. For PYTHIA the amount of multiple parton scattering depends on the parton distribution functions (*i.e.*, the structure functions) and hence the number of particles produced in the “transverse” region (*i.e.*, the “underlying event”) changes if one changes the structure functions. HERWIG and ISAJET do not include multiple parton scattering and for them the number of particles in the “transverse” is essentially independent of the choice of structure functions.

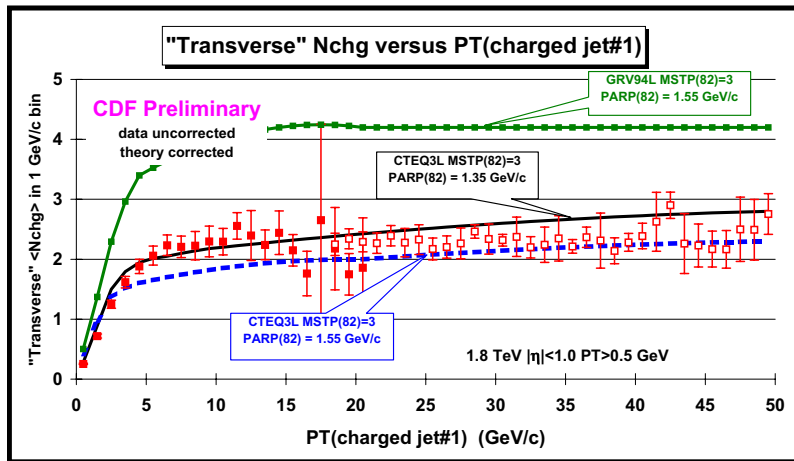


FIG. 22: Data on the average number of charged particles ($p_T > 0.5 \text{ GeV}/c$, $|\eta| < 1$) in the “transverse” region as a function of the transverse momentum of the leading charged jet compared with the QCD Monte-Carlo predictions of PYTHIA 6.115 with different structure functions and different multiple parton interaction parameters and with $p_T(\text{hard}) > 0 \text{ GeV}/c$. The theory curves are corrected for the track finding efficiency and have an error (*statistical plus systematic*) of around 5%.

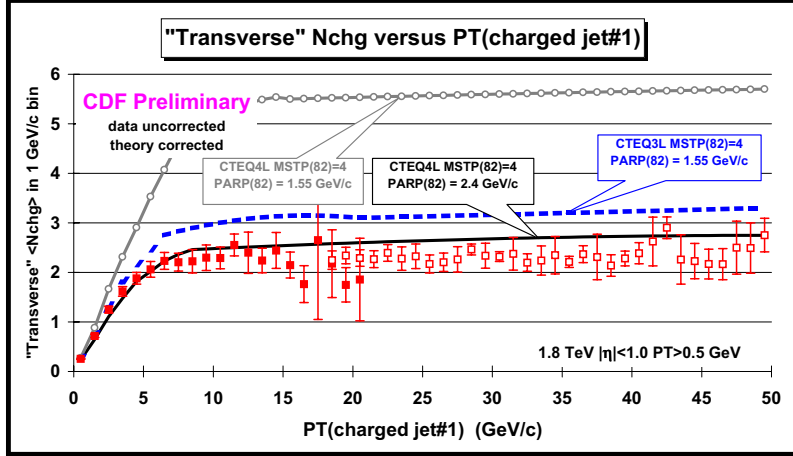


FIG. 23: Data on the average number of charged particles ($p_T > 0.5 \text{ GeV}/c$, $|\eta| < 1$) in the “transverse region as a function of the transverse momentum of the leading charged jet compared with the QCD Monte-Carlo predictions of PYTHIA 6.115 with different structure functions and different multiple parton interaction parameters and with $p_T(\text{hard}) > 0 \text{ GeV}/c$. The theory curves are corrected for the track finding efficiency and have an error (*statistical plus systematic*) of around 5%.

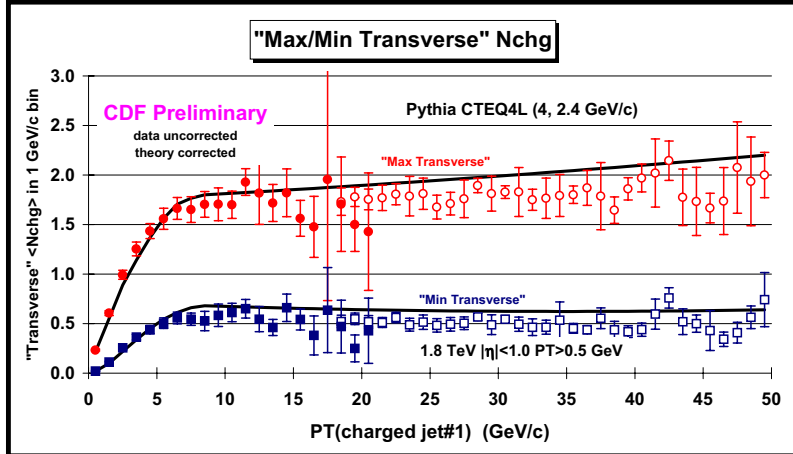


FIG. 24: Data on the average number of “transMAX” and “transMIN” charged particles ($p_T > 0.5 \text{ GeV}/c$, $|\eta| < 1$) as a function of the transverse momentum of the leading charged jet defined compared with the QCD Monte-Carlo predictions of PYTHIA 6.115 (*tuned version*, CTEQ4L, MSTP(82) = 4, PARP(82) = 1.4 GeV/c, $p_T(\text{hard}) > 0 \text{ GeV}/c$). The theory curves are corrected for the track finding efficiency and have an error (*statistical plus systematic*) of around 5%.

FIGS. 24- 29 show the results of a “tuned” version of PYTHIA 6.115 with $\text{MSTP}(82) = 4$ and $\text{PARP}(82) = 2.4 \text{ GeV}/c$ using the CTEQ4L structure functions. One must first choose a structure function and then tune the multiple parton scattering parameters for that structure function. In generating the PYTHIA curves in FIGS. 24- 29 we have taken $p_T(\text{hard}) > 0 \text{ GeV}/c$. In general the perturbative 2-to-2 parton scattering subprocesses diverge as $p_T(\text{hard})$ goes to zero. PYTHIA regulates these divergences using the same cut-off parameters that are used to regulate the multiple parton scattering cross section (see Table I). This allows for the possibility of using PYTHIA to simultaneously describe both “soft” and “hard” collisions. Most of the CDF Min-Bias events are “soft”, with less than 3% of the events having $P_T(\text{chjet}\#1) > 5 \text{ GeV}/c$. There is no clear separation between “soft” and “hard” collisions, but roughly speaking $P_T(\text{chjet}\#1) < 2 \text{ GeV}/c$ corresponds to “soft” Min-Bias collisions and demanding $P_T(\text{chjet}\#1) > 5 \text{ GeV}/c$ assures a “hard” collision. FIGS. 24- 27 show that the “tuned” version of PYTHIA with $p_T(\text{hard}) > 0 \text{ GeV}/c$ describes fairly well the transition between “soft” and “hard” collisions. The QCD Monte-Carlo models with $p_T(\text{hard}) > 3 \text{ GeV}/c$ cannot describe the data for $P_T(\text{chjet}\#1) < 3 \text{ GeV}/c$ (see FIG. 5 and FIG. 6), whereas PYTHIA with $p_T(\text{hard}) > 0 \text{ GeV}/c$ seems to do a good job on the “transverse” observables as $P_T(\text{chjet}\#1)$ goes to zero.

FIG. 28 shows the data on the transverse momentum distribution of charged particles in the “transverse” region compared with the “tuned” version of PYTHIA 6.115 (CTEQ4L, MSTP(82) = 4, PARP(82) = 2.4 GeV/c).

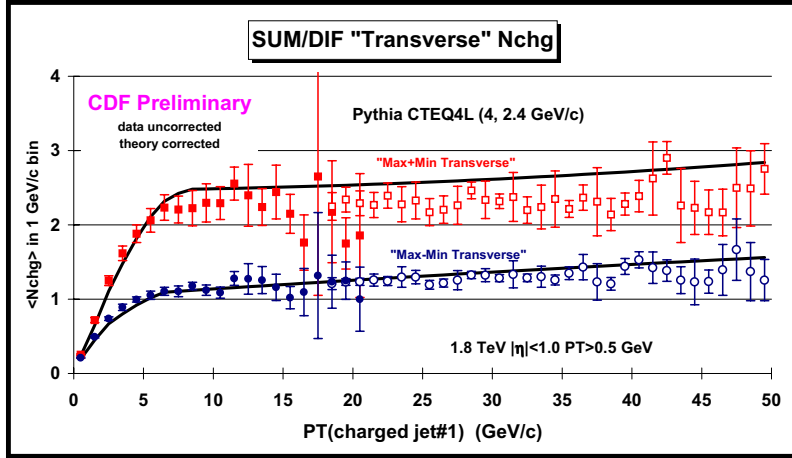


FIG. 25: Data on the average sum, “transMAX” plus “transMIN”, and difference, “transMAX” minus “transMIN” for the number of charged particles ($p_T > 0.5 \text{ GeV}/c$, $|\eta| < 1$) as a function of the transverse momentum of the leading charged jet defined compared with the QCD Monte-Carlo predictions of PYTHIA 6.115 (*tuned version*, CTEQ4L, MSTP(82) = 4, PARP(82) = 1.4 GeV/c, $p_T(\text{hard}) > 0 \text{ GeV}/c$). The theory curves are corrected for the track finding efficiency and have an error (*statistical plus systematic*) of around 5%.

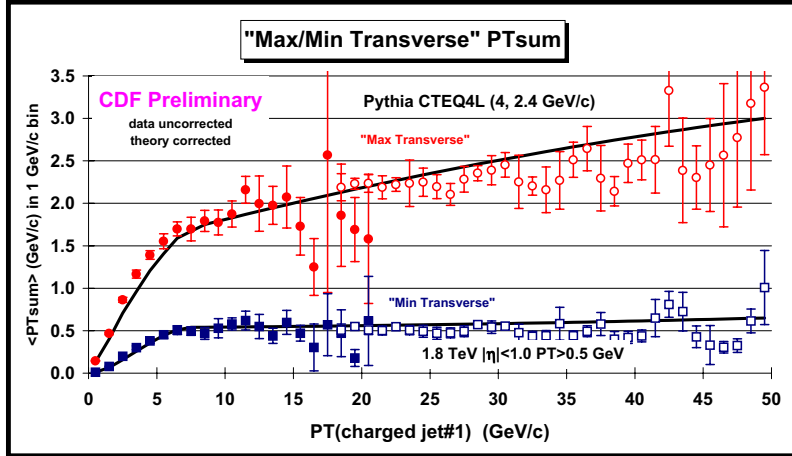


FIG. 26: Data on the average *scalar* p_T sum of “transMAX” and “transMIN” charged particles ($p_T > 0.5 \text{ GeV}/c$, $|\eta| < 1$) as a function of the transverse momentum of the leading charged jet defined compared with the QCD Monte-Carlo predictions of PYTHIA 6.115 (*tuned version*, CTEQ4L, MSTP(82) = 4, PARP(82) = 1.4 GeV/c, $p_T(\text{hard}) > 0 \text{ GeV}/c$). The theory curves are corrected for the track finding efficiency and have an error (*statistical plus systematic*) of around 5%.

The fit is not perfect, but it is much better than the HERWIG prediction shown in FIG. 17. Multiple parton scattering produces more large p_T particles in the “transverse” region, which is what is needed to fit the data. As seen in FIG. 29, the p_T distribution in the “transverse” region, at low values of $p_T(\text{chjet}\#1)$, for the “tuned” version of PYTHIA is also dominated by the “beam-beam remnant” contribution as is the case for HERWIG (see FIG. 18). However, for PYTHIA the “beam-beam remnant” component includes contributions from multiple parton scattering, which results in a less steep p_T distribution.

VII. SUMMARY AND CONCLUSIONS

The “underlying event” in a hard scattering process is a complicated and interesting object which involves aspects of both non-perturbative and perturbative QCD. Studying the “transMAX” and “transMIN” pieces of the “transverse” region provides additional information not contained in the sum. In the QCD Monte-Carlo models the various components that make up the “underlying event” are weighted differently in “transMAX” and “transMIN” terms. The “transMAX” term preferentially selects the “hard component” of the “underlying

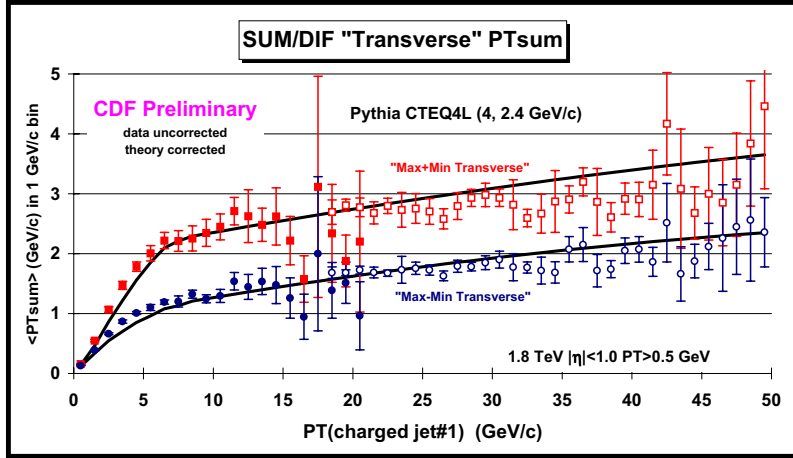


FIG. 27: Data on the average sum, “transMAX” plus “transMIN”, and difference, “transMAX” minus “transMIN” for the scalar p_T sum of charged particles ($p_T > 0.5 \text{ GeV}/c$, $|\eta| < 1$) as a function of the transverse momentum of the leading charged jet defined compared with the QCD Monte-Carlo predictions of PYTHIA 6.115 (*tuned version*, CTEQ4L, MSTP(82) = 4, PARP(82) = 1.4 GeV/c, $p_T(\text{hard}) > 0 \text{ GeV}/c$). The theory curves are corrected for the track finding efficiency and have an error (*statistical plus systematic*) of around 5%.

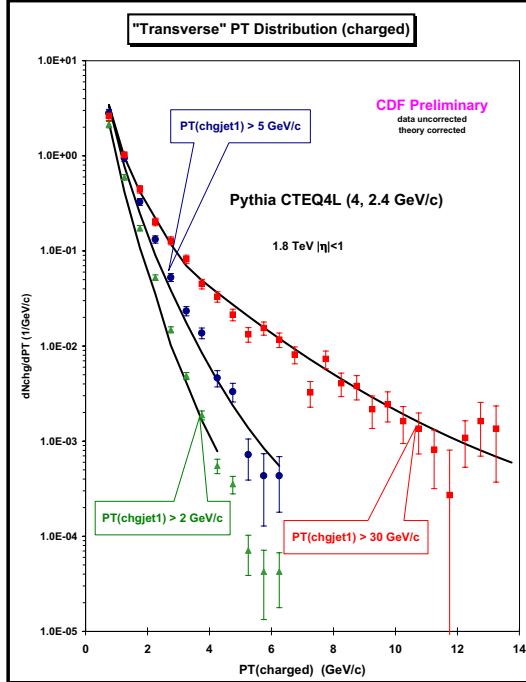


FIG. 28: Data on the transverse momentum distribution of charged particles ($p_T > 0.5 \text{ GeV}/c$, $|\eta| < 1$) in the “transverse region for $p_T(\text{chgjet}\#1) > 2 \text{ GeV}/c$, $5 \text{ GeV}/c$, and $30 \text{ GeV}/c$, where chgjet#1 is the leading charged particle jet. Each point corresponds to dN_{ch}/dp_T and the integral of the distribution gives the average number of charged particles in the transverse region, $\langle N_{ch}(\text{transverse}) \rangle$. The data are compared with the QCD Monte-Carlo model predictions of PYTHIA 6.115 (*tuned version*, CTEQ4L, MSTP(82) = 4, PARP(82) = 1.4 GeV/c, $p_T(\text{hard}) > 0 \text{ GeV}/c$). The theory curves are corrected for the track finding efficiency and have an error (*statistical plus systematic*) of around 5%.

event” (*outgoing jets plus initial and final-state radiation*) while the “transMIN” term preferentially selects the “beam-beam remnant” component. Unfortunately one cannot cleanly isolate a single component of the “underlying event” since all components contribute to both “transMAX”, “transMIN”, and to the difference. However, requiring the Monte-Carlo models to fit both “transMAX” and “transMIN” (or the sum and difference) puts additional constraints on the way the generators model the “underlying event”.

ISAJET (*with independent fragmentation*) produces too many (*soft*) particles in the “underlying event” with

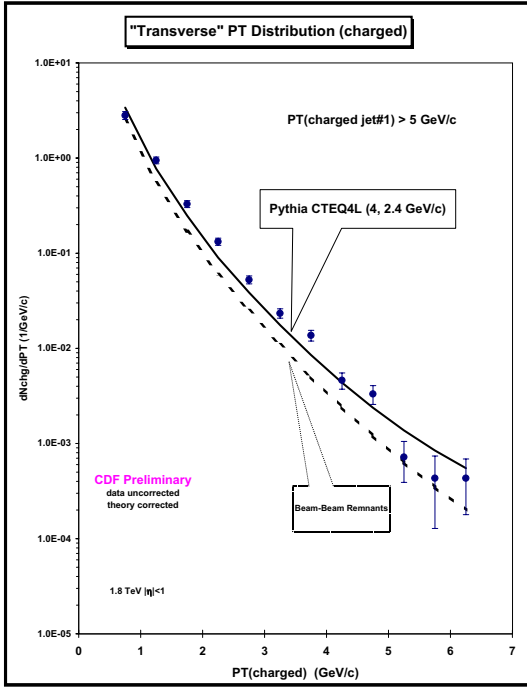


FIG. 29: Data on the transverse momentum distribution of charged particles ($p_T > 0.5 \text{ GeV}/c$, $|\eta| < 1$) in the “transverse region for $P_T(\text{chjet}\#1) > 5 \text{ GeV}/c$, compared with the QCD Monte-Carlo model predictions of PYTHIA 6.115 (*tuned version*, CTEQ4L, MSTP(82) = 4, PARP(82) = 1.4 GeV/c, $p_T(\text{hard}) > 0 \text{ GeV}/c$). The theory curves are corrected for the track finding efficiency and have an error (*statistical plus systematic*) of around 5%. The solid curve is the total (“hard scattering” plus “beam-beam remnants”) and the dashed curve shows the contribution arising from the break-up of the beam particles (“beam-beam remnants”). For PYTHIA the “beam-beam remnants” include contributions from multiple parton scattering.

the wrong dependence on $P_T(\text{chjet}\#1)$. HERWIG and PYTHIA modify the leading-log picture to include “color coherence effects” which leads to “angle ordering” within the parton shower and they do a better job describing the “underlying event”. Both ISAJET and HERWIG have the too steep of a p_T dependence of the “beam-beam remnant” component of the “underlying event” and hence do not have enough “beam-beam remnants” with $p_T > 0.5 \text{ GeV}/c$. PYTHIA with multiple parton scattering does the best job at fitting the data.

The increased activity in the “underlying event” of a hard scattering over that observed in “soft” collisions cannot be explained solely by initial-state radiation. Multiple parton interactions provide a natural way of explaining the increased activity in the “underlying event” in a hard scattering. A hard scattering is more likely to occur when the “hard cores” of the beam hadrons overlap and this is also when the probability of a multiple parton interaction is greatest. For a soft grazing collision the probability of a multiple parton interaction is small. However, multiple parton interactions are very sensitive to the parton structure functions (PDF). You must first decide on a particular PDF and then tune the multiple parton interactions to fit the data.

One should not take the “tuned” version of PYTHIA 6.115 (CTEQ4L, MSTP(82) = 4, PARP(82) = 2.4 GeV/c) presented here too seriously. It is encouraging that it describes fairly well the “transverse” region over the range $0 < P_T(\text{chjet}\#1) < 50 \text{ GeV}/c$ including the transition from “soft” to “hard” collisions. However, it is still not quite right. For example, it does not reproduce very well the multiplicity distribution of “soft” collisions. More work needs to be done in tuning the Monte-Carlo models [10]. In addition, more work needs to be done before one can say that the multiple parton interaction approach is correct. HERWIG without multiple parton scattering is not that far off the data. Maybe we simply need to change and improve the way the Monte-Carlo models handle the “beam-beam remnant” component.

[1] T. Sjostrand, Phys. Lett. **157B**, 321 (1985); M. Bengtsson, T. Sjostrand, and M. van Zijl, Z. Phys. **C32**, 67 (1986); T. Sjostrand and M. van Zijl, Phys. Rev. **D36**, 2019 (1987).

[2] *Charged Jet Evolution and the Underlying Event in Proton-Antiproton Collisions at 1.8 TeV*, The CDF Collaboration (T. Affolder et al.), FERMILAB-PUB-01/211-E.

- [3] *The Underlying Event in Large Transverse Momentum Charged Jet and Z-boson Production at 1.8 TeV*, talk presented by Rick Field at DPF2000, Columbus, OH, August 11, 2000.
- [4] *A Comparison of the Underlying Event in Jet and Min-Bias Events*, talk presented by Joey Huston at DPF2000, Columbus, OH, August 11, 2000. *The Underlying Event in Jet and Minimum Bias Events at the Tevatron*, talk presented by Valeria Tano at ISMD2001, Datong, China, September 1-7, 2001.
- [5] G. Marchesini and B. R. Webber, Nucl. Phys. **B310**, 461 (1988); I. G. Knowles, Nucl. Phys. **B310**, 571 (1988); S. Catani, G. Marchesini, and B. R. Webber, Nucl. Phys. **B349**, 635 (1991).
- [6] F. Paige and S. Protopopescu, BNL Report, BNL38034, 1986 (*unpublished*), version 7.32.
- [7] F. Abe *et al.*, Phys. Rev., **D41**, 2230 (1990).
- [8] *Hard Underlying Event Corrections to Inclusive Jet Cross-Sections*, Jon Pumplin, Phys. Rev. D57, 5787 (1998).
- [9] The latest versions of PYTHIA (6.120 and higher) include additional parameters that allow one to adjust the energy dependence of multiple parton interactions.
- [10] The latest version of HERWIG includes a multiple-parton scattering option, which can be tuned to fit the data presented here. See the Snowmass 2001 P5 talk by Jon Butterworth.